Ann. Geophysicae 16, 997–1006 (1998) © EGS – Springer-Verlag 1998

Annales Geophysicae

High resolution 2-D maps of OI 630.0 nm thermospheric dayglow from equatorial latitudes

D. Pallam Raju and R. Sridharan

Physical Research Laboratory, Ahmedabad 380 009, India

Received: 15 September 1997 / Revised: 27 February 1998 / Accepted: 16 March 1998

Abstract. The first-ever high resolution 2-D maps of OI 630.0 nm dayglow obtained from equatorial latitudes clearly reveal the movement as a large-scale feature of the equatorial ionization anomaly (EIA). These also show the presence of wave-like features classified as gravity waves presumably originating at the crest of the EIA, similar to the equatorial electrojet acting as a source of these waves. These results are presented and discussed.

Key words. Atmospheric composition and structure (Airglow and aurora) · Ionosphere (Equatorial ionosphere; Instruments and techniques).

1 Introduction

Both large- and small-scale processes extended in space and time continue to occur in the Earth's upper atmosphere as an outcome of the dynamical behaviour of the different regions responding to external energy inputs. This dynamical behaviour is engendered due to (a) the dissimilar energy inputs from the Sun which drive wind systems in the thermosphere and (b) the electrodynamical coupling within the thermosphere-ionosphere-system (TIS). In the equatorial TIS, the equatorial ionization anomaly (EIA) is a large-scale outcome of the dominant electrodynamical effects and extends to a latitudinal region of $\sim\pm$ 20° around the dip equator (Moffet, 1979). The EIA is generated by the E × B drift [$V_d = (E \times B)/B^2$] experienced by the plasma over the dip equator (where E and B are the electric and magnetic fields respectively) and its subsequent diffusion along the magnetic field lines to latitudes farther away from the dip equator (Martyn, 1947).

As the eastward electric field strength increases during the course of a day due to the intensification of global scale dynamo action, the drift, V_d, too, increases in consonance and the plasma which is lifted to higher heights is (eventually) transported poleward due to field aligned diffusion. This would then appear as the movement of the excess density in ionization (i.e. the 'crest'), in latitude with time and is generally referred to as the 'movement of the crest of the ionization anomaly'. These crests move away from the dip equator during the day and return towards the equator (the 'retrieval of the crest') during the night owing to the reversal in the polarity of the zonal electric field (Hanson and Moffet, 1966; Kulkarni, 1975; Agashe, 1987; Sridharan *et al.*, 1993). The development of the anomaly shows day-to-day as well as long period (such as season, solar cycle, etc.) variabilities.

One of the established techniques of investigating the EIA is by means of radio sounding of the ionosphere, both by bottomside and topside ionospheric sounders. (Croom *et al.*, 1959; King *et al.*, 1964; Sharma and Raghavarao, 1989). It is also seen in the latitudinal distribution of total electron content (TEC) (Rastogi and Klobuchar, 1990). Topside sounders have revealed significant longitudinal (spatial) differences as well (Walker *et al.*, 1980; Sharma and Raghavarao, 1989). This is in addition to the temporal variabilities mentioned earlier. Comprehensive reviews are available in the literature which deal with the overall morphology and large-scale variabilities of a EIA (Moffet, 1979; Raghavarao *et al.*, 1988; Sastri, 1990; Abdu *et al.*, 1991).

Though the gross features of the EIA are reasonably well understood, there are several intriguing aspects which call for further investigation. It not only affects the plasma distribution, but also alters the behaviour of neutrals as well. This was convincingly demonstrated by Hedin and Mayr (1973) who had shown using the data from OGO-6 that the neutral densities in the

Correspondence to: R. Sridharan *E-mail: sridhar@prl.ernet.in*

thermosphere showed an anomalous behaviour with latitude, with two crests and a trough collocated with that of the crests and trough of the EIA. This 'neutral anomaly' has been suggested by them to be possibly due to the excess ion-drag on the neutral zonal wind motion in the crest region of the EIA. Recent discoveries from the wind and temperature spectrometer (WATS) onboard the DE-2 satellite, (Raghavarao *et al*., 1991) have shown (1) an excess neutral temperature (of 50–100 K) over the crests of the EIA compared with its trough; and (2) enhanced zonal wind magnitudes (of $\sim$100 ms^{-1}) over the trough of the EIA compared to its crests. The discovery of the ETWA has encouraged renewed interest in EIA associated processes.

Other than the means mentioned for investigating the EIA and its associated processes, measurements of airglow emissions that emanate from the thermosphere have also been used, as the F-region electron densities have a significant control over those emissions (Barbier, 1963). As the observed airglow intensities are directly proportional to the electron densities, the variation in airglow intensity at different spatial locations at any given time indicates the position of the anomaly crest, and the spatial patterns at different times can be used to infer the movement of the same. Night-time detection of the EIA crests and their latitudinal movement had been made both by means of ground-based and satellite-borne optical detectors (Chandra *et al*., 1973; Kulkarni, 1975; Agashe, 1987). Though the satellites give good spatial coverage, they are restricted in providing information on the temporal evolution of a given phenomenon. Hence, it is essential that ground-based high-resolution imaging studies of the phenomenon be made to investigate the EIA dynamics from a single location. One such study was carried out recently by Sridharan *et al*., (1993) wherein they had used an all-sky Imaging Fabry-Perot Spectrometer to obtain the first two-dimensional high-resolution images of the OI 630.0 nm *nightglow* emission and they even estimated the equatorward velocity of the crest of the EIA to be $\sim$40 ms^{-1}. All such measurements were restricted to night-time only. Optical measurements in daytime, during the evolutionary phase of the EIA, are expected to provide newer insight into the phenomenon and its various manifestations. Due to the electrodynamical coupling between the thermosphere and ionosphere, any wave activity generated by movement of the EIA crest would modulate both the neutral and ion densities and hence, optical mapping of the EIA features would enable us to decipher many of these finer aspects.

Ever since the unique Dayglow Photometer (DGP) (Narayanan *et al*., 1989; Sridharan *et al*., 1992a) was commissioned, it was put in operation to detect the OI 630.0 nm dayglow emission intensities from various latitudinal locations of the Indian sub-continent. Many new results showing the semblance of OI 630.0 nm dayglow with electron density (Sridharan *et al*., 1991), the temporal variabilities and their causative mechanisms (Sridharan *et al*., 1992b), obtaining a precursor to the enigmatic ESF phenomena in OI 630.0 nm dayglow (Sridharan *et al*., 1994) and some of the first results on the development of the equatorial ionization anomaly by meridional scanning (Pallam Raju *et al*., 1996) have already been reported in the literature. From these studies, it was concluded that the temporal variations in the OI 630.0 nm dayglow at any location, are strongly controlled by the electron densities at that location and this has been successfully used in inferring the electrodynamical processes (Pallam Raju, 1996; Pallam Raju *et al*., 1996). The dayglow photometer has since been augmented with azimuth and elevation angle scanners and is now capable of mapping dayglow intensities. In this study we present the first two-dimensional high-resolution maps of OI 630.0 nm dayglow emission intensities obtained from equatorial stations in India, and these results clearly reveal the development of the EIA and the associated features along with its dynamics with unprecedented spatial and temporal resolution.

2 Instrumentation

Narayanan *et al*. (1989) described a method by which faint emission features buried in the strong background continuum of the daytime sky could be detected. This instrument, the dayglow photometer, employs a temperature-tuned narrow band-width (0.3 nm FWHM) interference filter followed by a pressure-tuned Fabry-Perot etalon of free spectral range of 0.4 nm. The pressure inside the FP chamber is maintained to better than 5% under tuned conditions, all through the day. Since it is a low resolution FP etalon (500 μm gap), any changes in the refractive index due to the temperature variations during the course of the day do not affect the tuning conditions. The FP fringe system is focused on to a unique mask assembly (Sridharan *et al*., 1992a) that consists of stationary (stator) and rotating (rotor) masks mounted concentrically. These masks consist of transparent and opaque regions and when the rotor concentrically rotates over the stator, light is periodically allowed from inner and outer annular zones. For the optical design of the DGP, the radial separation of the inner and outer zones brings about a change of $\sim$0.07 nm in wavelength domain due to the spatial dispersion property of the Fabry-Perot interferometer. The light that is allowed from the inner and outer zones at short intervals ($\sim$20 ms) is refocused on to a thermo-electrically cooled photomultiplier tube. The counts from the two counters corresponding to the inner and outer zones are counted separately and are incremented synchronously with the rotor positions. Under a tuned condition of the FP, the counts from the inner annular zone would represent the contribution from the OI 630.0 nm emission as well as from the scattered background (at that wavelength) and those from the outer zone would represent the contribution due to background alone (separated by just $\sim$0.07 nm). As mentioned earlier, these are integrated typically for 20 s duration after which they are subtracted to yield the contribution of OI 630.0 nm dayglow intensity alone. The estimated uncertainties are 10–20% for the absolute intensity over a day and better than 2% for variabilities

of the order of >30 min. These intensities are plotted online on the PC monitor and are also simultaneously stored. This instrument has been augmented with azimuth and elevation angle scanners recently. The movement of these scanners has been achieved by using stepper motors which in turn are controlled by the PC. The number of directions (either elevation or azimuth) to be scanned and the number of data points to be collected at each direction are all chosen by means of menu-driven software.

Care had been taken to operate the instrument in an all sky mode only during clear sky conditions. Since the FP is an imaging device, the presence of a wisp of sunlit cloud would preferentially modulate the background zone and/or the signal + background zone, depending upon the region where it is present. This would cause a sudden jump either way resulting in a discontinuity at the time of mapping. Further, the presence of fine Fraunhofer absorption features in the solar background and the telluric absorption features in addition to the Ring effect, due to the atmospheric constituents do not affect the relative intensity measurements reported here. This aspect has been amply demonstrated experimentally and discussed extensively by Narayanan *et al.*, (1989) and Sridharan *et al.*, (1998). It had been shown by them that these features, if any, present in the spectral windows get smoothed out due to the large window (0.07 nm) and also due to the large field of view (2–3°). Any imbalance is also accounted for while balancing the photometer for appropriate background rejection using the electronic gate widths. The quick sampling time of 10 ms also helps in overcoming these difficulties. It has also been ensured that direct sunlight does not enter into the instrument during the course of its operation.

3 Data presentation and analysis

It is well known that the OI 630.0 nm dayglow emission consists of three main sources, i.e. (a) photoelectron impact on atomic oxygen, (b) photo-dissociation of molecular oxygen and (c) dissociative recombination of O_2^+ with ambient electrons (Hays *et al.*, 1978). It has been shown by earlier studies that the temporal variability in dayglow is governed solely by the dissociative recombination mechanism (Sridharan *et al.*, 1991; 1992b). Using this fact and by employing meridional scanning of the dayglow intensities, the temporal evolution of the EIA was tracked using the DGP (Pallam Raju *et al.*, 1996).

After the augmentation of an azimuthal scanner, the DGP was operated in a campaign mode from two equatorial stations i.e. Waltair (17.7 N, 83.3°E; 10.0°N dip latitude and Tirupati (13.65°N, 79.41°E; 5.5°N dip latitude during January to March 1995 and the first-ever 2-dimensional maps of OI 630.0 nm *dayglow* intensities have been obtained. The choice of these two stations were made based on the prevailing low solar activity levels as, during this extremely quiet period of the Sun, the EIA and the associated effects on the thermosphere-ionosphere system are known to be confined to latitudes closer to the dip equator than during high solar activity periods. Data were obtained for ten clear sky days. The scan was performed in the following azimuthal directions: N, NW, W, SW, S, SE, E and NE. At each azimuth angle, data were obtained from four elevation angles i.e., 30°, 40°, 50° and 90° (zenith). So the largest distance that could be covered with 30° elevation angle (for an emission height of 250 km) turns out to be ~4° in latitude and hence the spatial coverage is of 8° latitude × 8° longitude. For an integration time of 20 s per datum point, a two-dimensional map was obtained in just 12 min.

3.1 Removal of solar glare effect

In all-sky scanning mode, the dayglow photometer comes across some regions in the direction of the Sun where solar background intensity has steep spatial gradients, which keep changing due to rotation of Earth during the interval of data collection. Though the data acquisition in the DGP between the signal + background and the background counters is in quick successions (of ~10 ms), the 'background' does not remain the same even in the 10 ms time interval especially in the direction towards the Sun and its surrounding regions. This has been observed experimentally and has been accounted for in the data analysis in the following way.

As mentioned earlier, the data acquisition is done for intensity values of signal and background in counter 1 and background alone in counter 2. Polynomial fits have been estimated for the values of these intensities separately for each of the 25 directions with time. If the 'uncontaminated' background is to be estimated for a given time t_1, then depending on the 'trend' of its intensity variation, i.e. with an increase or decrease in intensity with time, the background intensity level at a time (t_1 + 10 ms) or (t_1 − 10 ms) respectively is considered. This background intensity level so estimated is subtracted from the signal intensities (estimated at t_1 using the polynomial fit) to obtain the difference. An estimate of the differences made at neighbouring intervals of 10 ms each are integrated for 20 s, to simulate the actual condition and also to achieve better signal-to-noise ratio. This is amply demonstrated in Fig. 1 which shows a plot for one direction (30° elevation towards south) on 6 February 1995 as obtained from Waltair (10.0°N dip latitude) India. It can be seen that there is a steady increase of this solar glare and, especially during noontime, there is a maximum contribution which decreases in later part of the day. The intensity obtained after the removal of the solar glare by the mentioned method is also shown. One can see that the sudden and non-linear increase in the noontime has been taken into account appropriately. Such analysis is done for all the 25 directions of observations and 2-D plots have been obtained. Both surface and contour plots have been depicted which elucidate the development and characteristic features of the EIA.

4 Results

Figures 2 and 3 show a collage of typical hourly plots of the first two-dimensional maps of OI 630.0 nm dayglow emission intensity for 31 January and 6 February 1995 obtained from Waltair. As dictated by convention the topside of each plot in these figures indicates geographic north and the left side indicates the west. With a knowledge of the emission height and elevation angles of the instrument, it is straight-forward to calculate the respective projected distances of data collection from the point of observations. Knowing the coordinates of the observing station, these distances have been transformed into latitudes and longitudes. The spatial extent covered by these plots are 8° latitude × 8° longitude with the observational station at the centre. The coordinates corresponding to the observation are shown in the bottom and left hand sides of the plots. The time to which each plot corresponds is shown at the top-centre of each plot.

In the plot corresponding to 0830 h on 31 January 1995, it can be seen that the directions of east and southeast show higher intensity compared to the west. With progression of time, the region of excess intensity, i.e. the crest, gets formed and moves into the 'overall' range (8° latitude × 8° longitude) of the system. The plots of 1130 h to 1330 h clearly show the movement of these crests. As the temporal variations of OI 630.0 nm dayglow emission intensities are nearly identical to those observed in the electron densities, as has been demonstrated through coordinated photometric and ionosonde measurements from Mt. Abu (24.6°N, 73°E and 19°N dip latitude) and Ahmedabad (23°N, 72.6°E and 17°N dip latitude), (Sridharan *et al.*, 1992; Pallam Raju *et al.*, 1996), the 'movement' of the excess intensity is interpreted to be the movement of the EIA itself through the centroid of dayglow emission at ~250 km. During the course of the day this crest sweeps past the longitude of the observational station and moves towards the west and southwestern directions.

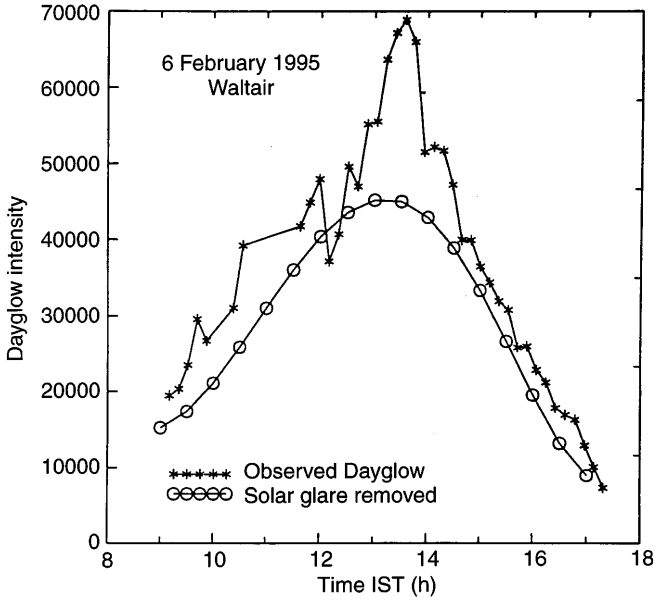

Fig. 1. Observed dayglow intensity (*stars*) and that corrected for solar glare (*circles*). The dayglow intensity corrected for solar glare can be seen to be distinctly different from the observed data (refer text for details)

Figure 3 (corresponding to 6 February) shows a similar behaviour as in Fig. 2 in terms of the movement of the large-scale feature, as expected. There are however, some differences which can be noticed in terms of the magnitude in intensities. The intensities on 6 February 95 are larger by nearly a factor of two compared to those on 31 January 1995.

It should be noted that these observations correspond to a low solar activity period during which the EIA development is expected to be weak. It is believed that for this reason and also due to the dayglow emission height being centred near 250 km the northernmost latitude to which the crest developed is just south of the observing location (at 10°N dip latitude). If such observations are carried out from a location southward of this station, they should show differences in the pattern of development of the EIA especially with regard to the location of the crest. Such an experiment was planned and carried out from Tirupati, an equatorial station (5.5°N dip latitude), during the month of March 1995. In Fig. 4 we show the data obtained on 13 March 1995. Here, in addition to similarities in the form of the movement of the EIA crest, many new features could also be seen. Some of them are that (1) the peak intensity contours (crest) are seen in a location northward of the station in the plots corresponding to 1230 h and 1330 h, (2) finer, cellular structures are seen within the crest region, (3) the longitudinal extent over Tirupati is larger than the one observed over Waltair (in terms of FWHM) and (4) there are distinct differences in the evolutionary patterns. From Figs. 2 and 3 it can be noticed that seen from the observational location (Waltair), the crest of the EIA *arrives* from the southeast in the morning and *departs* towards the southwest in the evening. Meanwhile, it can be seen from Fig. 4, corresponding to Tirupati, that the crest moves from east to west (with only a very small component in the south-eastern and southwestern directions) in the morning and evening hours respectively. This is what one would expect at a location directly beneath the anomaly crest for longer time during a day.

Figures 5 and 6 show the surface plots of 630.0 nm dayglow intensity variation for 1 and 11 February 1995 as observed from Waltair. In this representation the $x-$, $y-$ and $z-$ axes represent longitude, dip latitude and intensity respectively. Time is shown on the top left corner of each plot. Here too, it can be seen that the crest moves from the south-east to the south-west. Figure 7 shows the data obtained from Tirupati on 15 March 1995 presented in similar lines. The differences in the intensities between the two observing locations and between two points in the same plot are brought out clearly in this representation. One can notice wavy and curtain-like features indicating the presence of wavelengths of ~2° in latitude (~200 km). Such wave-like

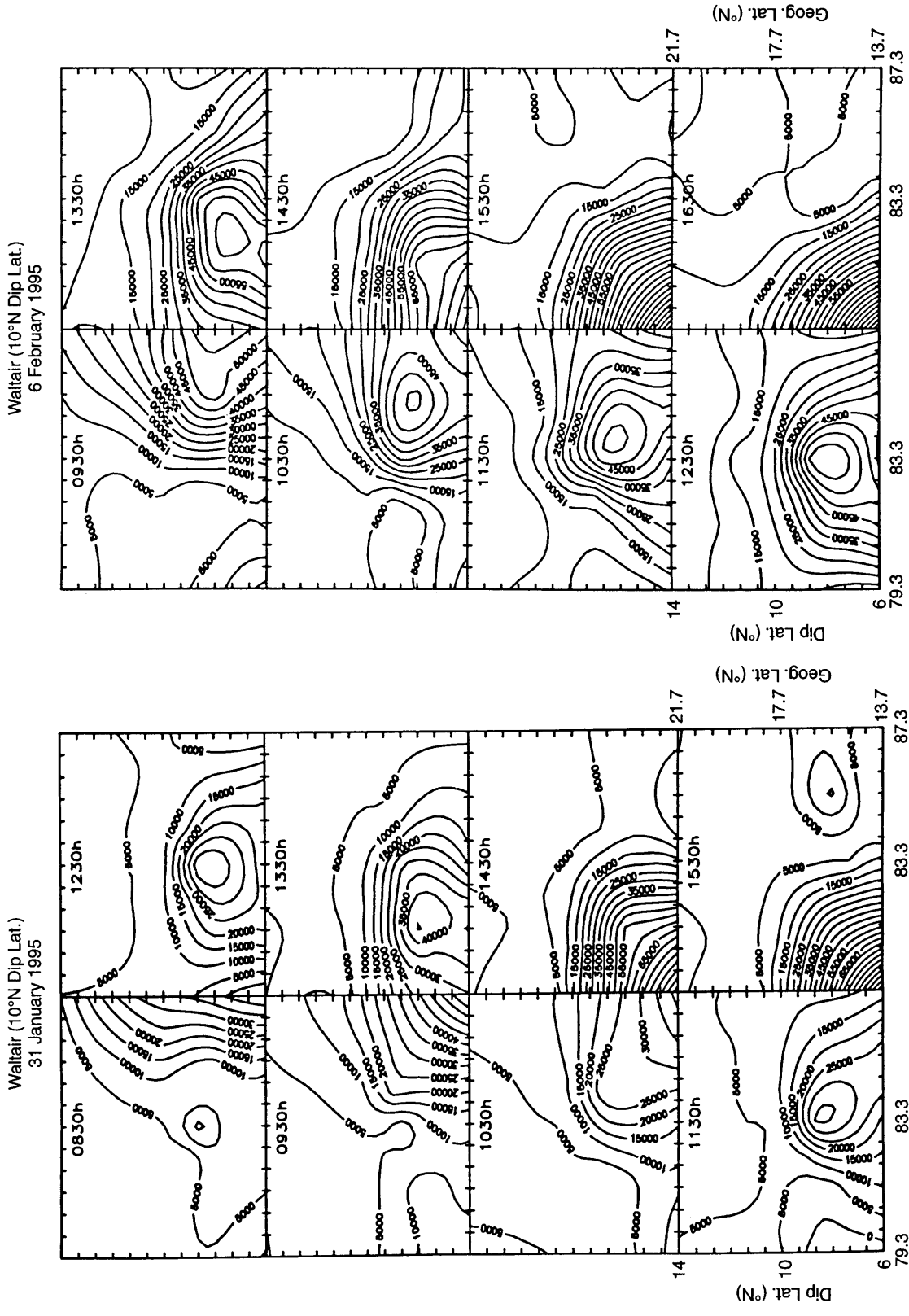

Fig. 2. Collage of hourly plots of 2-D maps of OI 630.0 nm dayglow for 31 January, 1995 obtained from Waltair (10.0°N dip latitude) after the glare correction

Fig. 3. Same as in Fig. 2 but for 6 February 1995

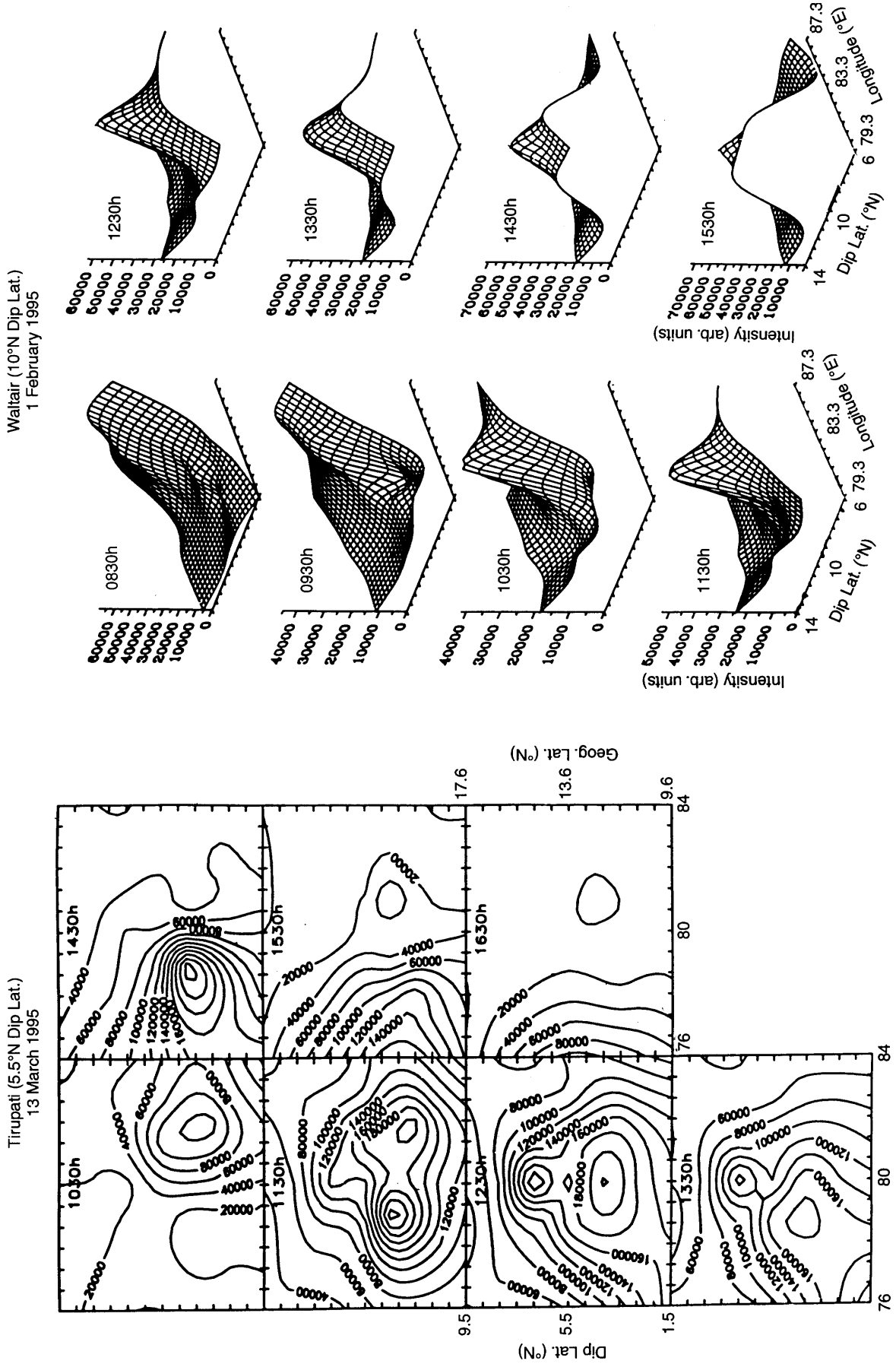

Fig. 4. Same as in Fig. 2 but for 13 March 1995 obtained from Tirupati (5.5°N dip latitude), a station closer to the dip equator

Fig. 5. Surface plots of OI 630.0 nm dayglow emission on 1 February 1995 obtained from Waltair

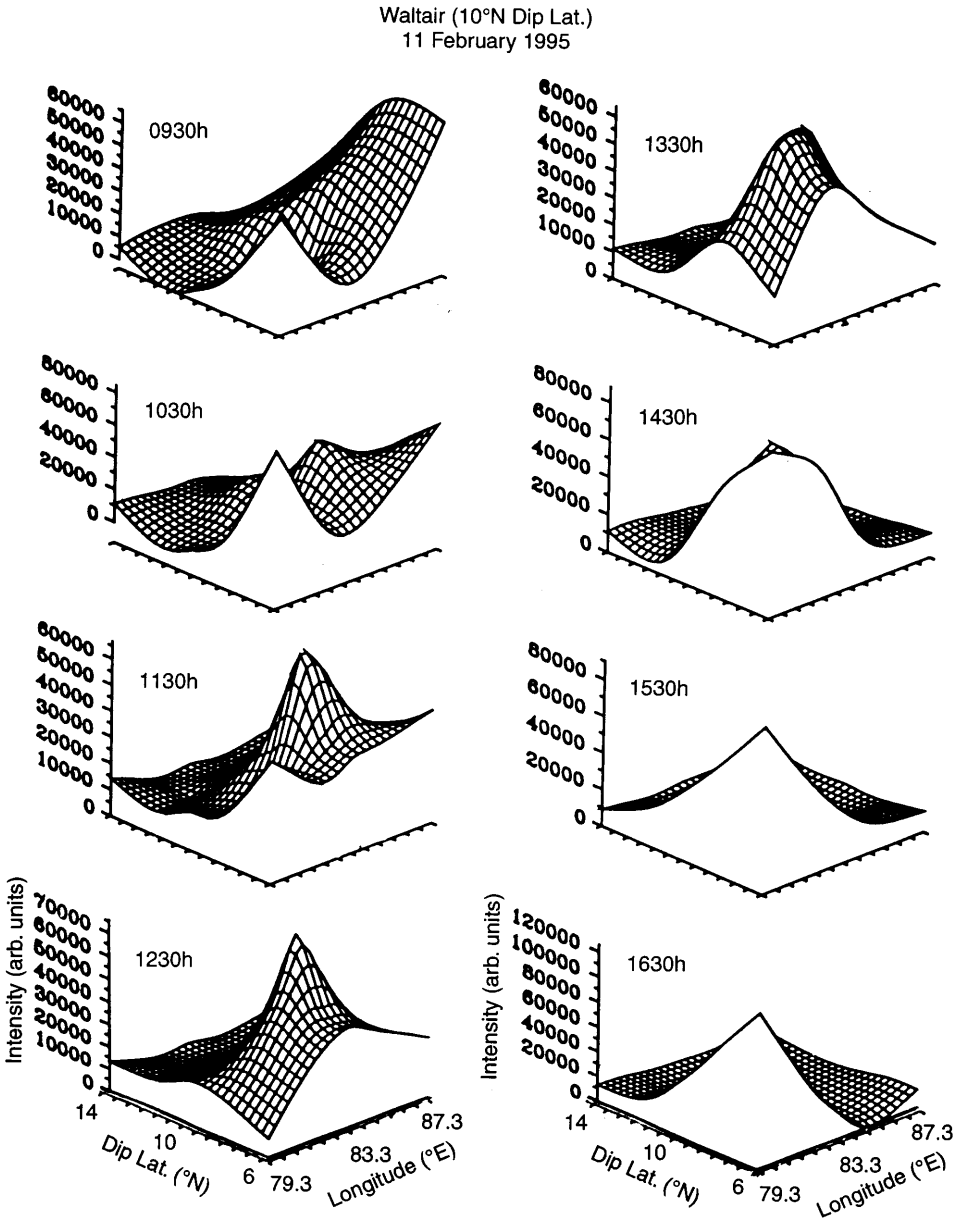

Fig. 6. Same as in Fig. 5 but for 11 February 1995

and cellular structures become clearer in the contour plot with smaller intensity separation. Figure 8 shows one such plot obtained from Waltair on 11 February 1995 at 1730 h. A wavy structure oriented in the northeast direction with a crest at ~7 and a trough at 10.5 degree dip latitude can be seen. There is a tendency for a build up beyond 14° dip latitude. The scale-size of the structure is of the order of 800 km.

5 Discussion

One of the important aspects when the photometer is operated in an all sky mode, is to ensure that the spatial structures presented are not an artefact and are real. This becomes all the more important when the region being sampled has varying background intensities. The position of the Sun is southward to the location of observations during the period of under consideration i.e. from January to March. Though the development of EIA and the local time variation of the peak of EIA is solar zenith angle dependent, the fact that the EIA peak is overhead or even north of Tirupati is strong evidence that an uncorrected solar glare and the perceived EIA maximum are not the same thing.

Further it is known that at upper atmospheric heights, quite a few wave phenomena get engendered due to (1) differential inputs of solar energy; (2) various local sources of additional energy from below; (3) high-latitude energy sources, especially during magnetic storms, etc. In addition, it has been shown by Chimonas (1970) that equatorial phenomena like the equatorial electrojet (EEJ) can give rise to gravity waves during the course of their development. A similar possibility does exist with regard to the EIA also, as the wave structures seen in Figs. 2–8 suggest that they originate near the

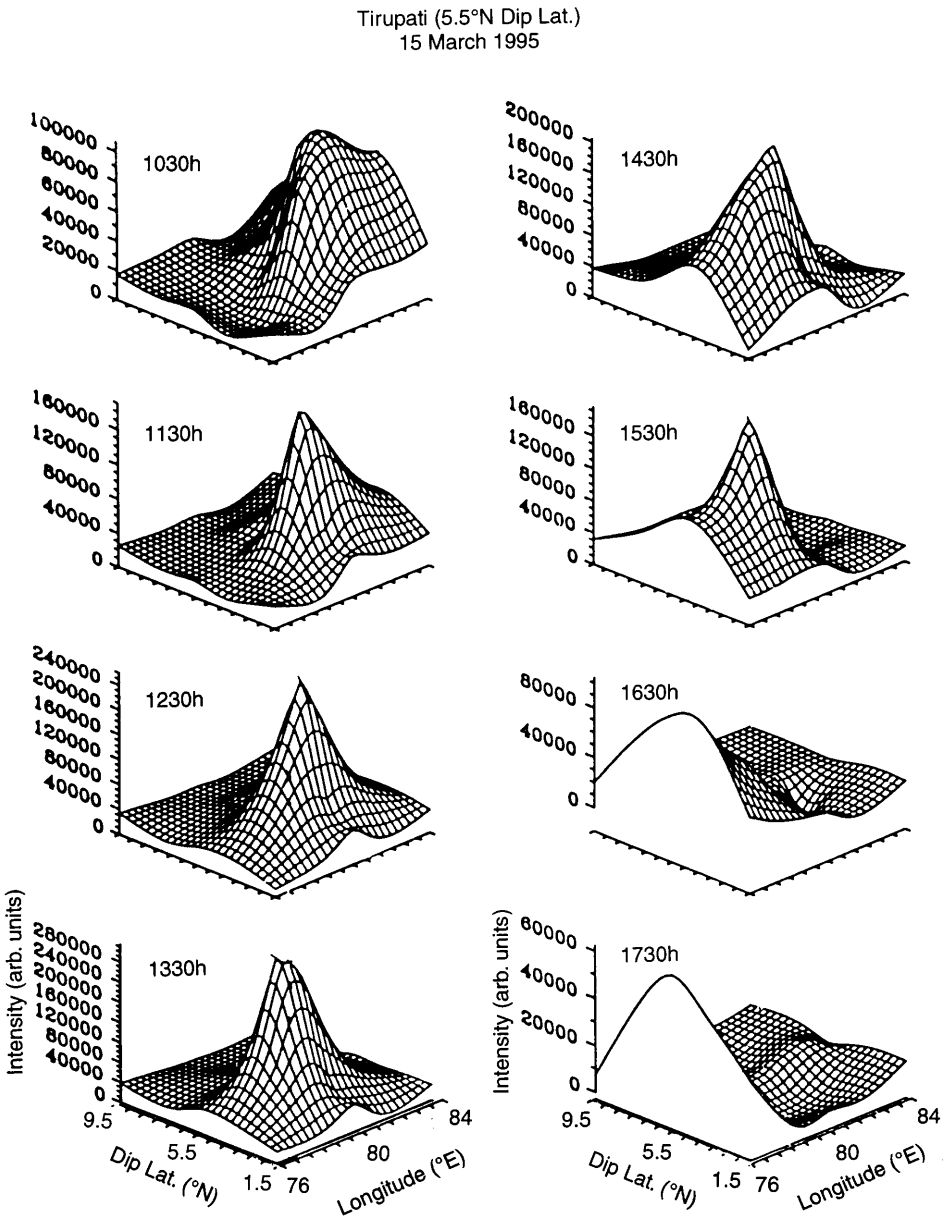

Fig. 7. Same as in Fig. 5 but for 15 March 1995 obtained from Tirupati

crest of the EIA and their horizontal scale-size falls into the class of gravity waves. The frequency of occurrence of such waves is difficult to estimate at this time because very limited data are available at the local times when such waves are seen. The waves appear only when the background levels are low, implying that their amplitudes are considerably smaller than midday background levels. Typically these wave amplitudes would form $<1\%$ of the noontime dayglow intensity which itself is $<5\%$ of the background intensities. This explains why they appear prominently only during evening hours and why probably the nightglow photometers have shown these wave activities preferentially (Takahashi *et al.*, 1989; Sobral *et al.*, 1981). Further, when such maps are obtained from the dip equator, extending to twilight times, the characteristic features such as the scale length of the initial perturbations and also their amplitudes which could eventually trigger the equatorial spread-F could be obtained. The observation of such waves by conventional radio probing methods requires a chain of stations separated by a very short distance (of the order of $\sim 1°$ in latitude). The present study demonstrates that the 2-D maps of OI 630.0 nm dayglow measurements enable the investigation of such wave phenomena. More intensive campaigns are planned to characterise the wave phenomena apart from studying the evolutionary characteristics of EIA and its variabilities and also of the phenomenon of equatorial spread-F

When one is investigating the evolution of the EIA, it should be borne in mind that its development in intensity and latitudinal movement is essentially due to the zonal electric field and the thermospheric wind-assisted plasma diffusion along the geomagnetic field. The plasma velocity $\mathbf{V}$ at any instant is made up of the electromagnetic drift velocity $\mathbf{V} = \mathbf{E} \times \mathbf{B}/\mathbf{B}^2$, the ambipolar diffusion velocity V_{diff} and a neutral component

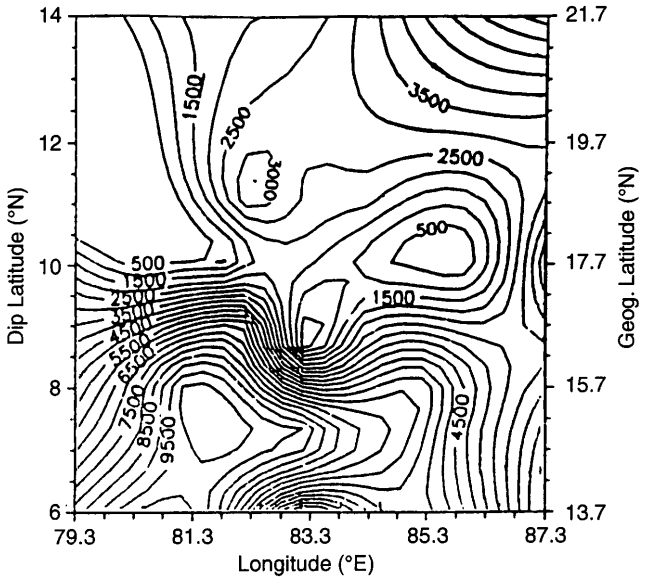

Fig. 8. A 2-D map obtained from Waltair on 11 February 1995 at 1730 h. Wave-like feature (possibly associated with the crest of EIA) with scale size ranging ~ 800 km in the northeastern direction could be clearly seen

velocity ($\mathbf{U}.\mathbf{B}/\mathbf{B}^2$) where $\mathbf{B}$ is the magnetic field and U is the neutral velocity. Thus,

$$\mathbf{V} = \mathbf{V}_{\text{diff}} + \left(\frac{\mathbf{U}.\mathbf{B}}{\mathbf{B}^2}\right) + \frac{\mathbf{E} \times \mathbf{B}}{\mathbf{B}^2}$$

The role of the electromagnetic drift in the generation of the EIA has been investigated by Bramley and Peart (1964), while the neutral wind effects have been studied by Hanson and Moffet (1966). Rishbeth (1967) investigated in detail the role of plasma diffusion in EIA evolution. The role of ambipolar diffusion has been studied in detail by Sivaraman *et al.* (1976) who provided a viable explanation for the observed differences between solar maximum and minimum by solving the time dependent continuity equation.

From this discussion, it is clear that, quantification of the relative importance of electric fields and winds would require simultaneous data and any observation through airglow could yield only a representative, integrated picture of the evolution of EIA. However, since the observational period is during the same season and solar epoch of low solar activity conditions and also represent geomagnetically quiet periods, the thermospheric winds are not expected to vary drastically from one day to another (Hedin *et al.*, 1988; Hedin 1991). Under these circumstances, the variability revealed by the EIA as seen in OI 630.0 nm dayglow would correspond to the electric field variability. The dayglow maps could then be used to infer the spatial and temporal variability of the electric field itself. More detailed investigation in this direction is called for.

Conclusions

The OI 630.0 nm (neutral) dayglow emission serves as a good indicator for investigating the processes of the ionosphere owing to the thermosphere-ionosphere coupling. Measurement of these emissions by the unique dayglow photometer resulted in obtaining the first two-dimensional maps with a temporal resolution of ~12 min and these maps revealed the evolution of the EIA, including the movement of its crests and its spatial extent. Spatial structures as small as $1° \times 1°$ in latitude, longitude and wave-like features, presumably originating at the crest of the EIA, have also been detected. These measurements demonstrate the potential of the daytime technique in the investigation of wave-like phenomena in general and associated with the geophysical processes like EIA in particular.

Acknowledgements. We gratefully acknowledge Prof. D. R. K. Rao and the Director, Indian Institute of Geomagnetism for providing logistic support to carry out the dayglow observations from their Magnetic Observatory in Waltair. Our thanks are also due to Prof. P. B. Rao, Director, National MST Radar Facility, Tirupati for extending logistic support to carry out the measurements from Tirupati. This work is supported by the Department of Space, Government of India.

Topical Editor D. Alcayde′ thanks R. Link and R. Wiens for their help in evaluating this paper.

References

Abdu, M. A., J. H. A. Sobral, E. R. De Paula, and I. S. Batista, Magnetospheric disturbance effects on the equatorial ionization anomaly (EIA): an overview, *J. Atmos. Terr. Phys.*, **53**, 757, 1991.

Agashe V. V., Airglow studies in India, *Ind. I. Radio and Space Phys.* **16**, 84, 1987.

Barbier, D., Etude de la couche F d'apres l'emission de la raie rough du ciel nocturne, *Planet. Space Sci.*, **16**, 29, 1963.

Bramley, E. N., and M. Peart, Diffusion and electromagnetic drift in the equatorial F_2-region, *J. Geophys. Res.*, **69**, 4609, 1964.

Chandra, S., E. I. Reed, B. E. Troy Jr., and J. E. Blamont, Equatorial airglow and ionospheric geomagnetic anomaly, *J. Geophys. Res.*, **78**, 4630, 1973.

Chimonas, The equatorial electrojet as a source of long period travelling ionospheric disturbances, *Planet. Space Sci.*, **18**, 583–589, 1970.

Crooms, S. A., A. Robbins, and J. O. Thomas, Two anomalies in the behaviour of the F_2 layer of the ionosphere, *Nature*, **184**, 2003, 1959.

Hanson, W. B., and R. J. Moffet, Ionization transport effects in the equatorial F region, *J. Geophys. Res.*, **71**, 5559, 1966.

Hays, P. B., D. W. Rusch, R. G. Roble, and J. C. G. Walker, The OI (6300 A) airglow, *Rev. Geophys.*, **16**, 225, 1978.

Hedin, A. E., Revised global model of thermospheric winds, using satellite and groundbased observations, *J. Geophys. Res.*, **96**, 7657, 1991.

Hedin, A. E., and Mayr, H. G., Magnetic control of the near equatorial neutral atmosphere, *J. Geophys. Res.*, **78**, 1688, 1973.

Hedin, A. E., N. W. Spencer, T. L. Killeen, Empirical global model of upper thermospheric winds based on Atmospheric and Dynamics Explorer satellite data, *J. Geophys. Res.*, **93**, 9959, 1988.

King, J. W., P. A. Smith, D. Eccles, G. F. Fooks, and H. Helm, Preliminary investigation of the structure of the upper

atmosphere as observed by the topside sounder satellite, Alouette, *Proc. R. Soc.*, *London*, **281**, 464, 1964.

Kulkarni, P. V., 6300 Å night airglow and the geomagnetic control of the equatorial anomaly, *Proc. Indian Acad. Sci. Earth Planet. Sci.*, **82**, 46, 1975.

Martyn, D. F., Atmospheric tides in the ionosphere, I, Solar tides in the F_2 region, *Proc. R. Soc. London*, **A189**, 241, 1947.

Moffet, R. J., The equatorial anomaly in the electron distribution of the terrestrial F region, *Fund. Cosmic. Phys.*, **4**, 313, 1979.

Narayanan, R., J. N. Desai, N. K. Modi, R. Raghavarao and R. Sridharan, Dayglow photometry: a new approach, *Appl. Opt.*, **28**, 2138, 1989.

Pallam Raju, D., Studies of daytime upper atmospheric phenomena using groundbased optical techniques, *Ph.D Thesis*, Devi *Ahilya University*, *Indore*, *India*, 1996.

Pallam Raju, D., R. Sridharan, S. Gurubaran and R. Raghavarao, First results from ground-based daytime optical investigations of the development of equatorial ionization anomaly, *Ann. Geophysicae*, **14**, 238, 1996.

Raghavarao, R., R. Sridharan, J. H. Sastri, V. V. Agashe, B. C. N Rao, P. B. Rao, and V. V. Somayajulu, The equatorial ionosphere – world ionosphere/thermospheric study, *WITS Handbook*, vol 1, **48**, 1989.

Raghavarao, R. L. E. Wharton, N. W. Spencer, H. G. Mayr, and L. H. Brace, An equatorial Temperature and wind anomaly (ETWA), *Geophys. Res. Lett.*, **18**, 1193, 1991.

Rastogi, R. G., and Klobuchar, J. A., Ionospheric electron content within the equatorial F_2 layer anomaly belts, *J. Geophys. Res.*, **95**, 19045, 1990.

Rishbeth, H., The effects of winds on ionospheric F_2 peak, *J. Atmos*, *Terr. Phys.*, **29**, 225, 1967.

Sastri, J. H., Equatorial anomaly in F-region – a review, *Indian J. Radio Space Phys.*, **19**, 225, 1990.

Sharma, P., and R. Raghavarao, Simultaneous occurrence of ionization ledge and counter electrojet in the equatorial ionosphere: its implications, *Can. J. Phys.*, **67**, 166, 1989.

Sivaraman, M. R., R. Suhasini, and R. Raghavarao, Role of ambipolar diffusion in the development of equatorial anomaly in solar maximum and minimum periods, *Ind. J. Rad. Space Sci.*, **5**, 136, 1976.

Sobral, J. H. A., M. A. Abdu, I. S. Batista, and C. J. J. Zamlutti, Wave disturbances in the low latitude ionosphere and equatorial ionospheric plasma depletions, *Geophys. Res.*, **86**, 1374, 1981.

Sridharan, R., R. Raghavarao, S. Gurubaran and R. Narayanan, First results of OI 630.0 nm dayglow measurements from equatorial latitudes, *J. Atmos. Terr. Phys.*, **53**, 521, 1991.

Sridharan, R., R. Narayanan, and N. K. Modi, An improved chopper mask design for the dayglow photometer, *Appl. Opt.*, **31**, 425, 1992a.

Sridharan, R., S. A. Haider, S. Gurubaran, R. Sekar and R. Narayanan, OI 630.0 nm dayglow in the region of equatorial ionization anomaly: Temporal variability and its causative mechanism, *J. Geophys. Res.*, **97**, 13715, 1992b.

Sridharan, R., R. Sekar and S. Gurubaran, Two dimensional high resolution imaging of the equatorial plasma fouantain, *J. Atmos. Terr. Phys.*, **55**, 1661, 1993.

Sridharan, R., D. Pallam Raju, R. Raghavarao and P.V.S. Ramarao, Precursor to equatorial spread-F in OI 630.0 nm dayglow, *Geophys. Res. Lett.*, **21**, 2797, 1994.

Sridharan, R., N. K. Modi, D. Pallam Raju, R. Narayanan, Taurn K. Pant, Alok Taori and D. Chakrabarty, Multiwavelength daytime photometer – a new tool for the investigation of atmospheric processes, to appear in *Measurement Science and Tech.* (UK), 1998.

Takahashi, H., Y. Sahai, B. R. Clemesha, D. M. Simonich, N. R. Teixeira, R. M. Lobo and A. Eras, Equatorial mesospheric and F. region airglow emission observed from latitude 4° south, *Planet. Space Sci.*, **37**, 649, 1989.

Walker, G. O., J. H. K. Ma, R. G. Rastogi, M. R. Deshpande and H. Chandra, Dissimilar form of the ionospheric equatorial anomaly observed in East Asia and India, *J. Atmos. Terr. Phys.*, **42**, 629, 1980.